Nucleic Acids Research, 2025, **53**, gkaf269
https://doi.org/10.1093/nar/gkaf269
Genome integrity, repair and replication

In vivo nucleotide excision repair by mycobacterial UvrD1 requires ATP hydrolysis but does not depend on cysteine disulfide-mediated dimerization and DNA unwinding

Garrett M. Warren and Stewart Shuman*

[1]Molecular Biology Program, Memorial Sloan Kettering Cancer Center, NY, NY 10065, United States
*To whom correspondence should be addressed: Email: shumans@mskcc.org

Abstract

Mycobacterial UvrD1 is an SF1-type ATPase that participates in nucleotide excision repair (NER). UvrD1 consists of N-terminal ATPase and C-terminal Tudor domains. The monomeric UvrD1 characterized originally displays vigorous DNA-dependent ATPase activity but only feeble helicase activity. A recent study demonstrated that: (i) cysteine disulfide-mediated homodimerization of UvrD1 generates a highly active helicase; and (ii) an obligate monomeric UvrD1 (by virtue of mutating the domain 2B cysteine) is active as an ATP-dependent 3′-to-5′ single-stranded DNA translocase but not as a double-stranded DNA-unwinding helicase. Here we test genetically which physical and functional states of UvrD1 are relevant for its functions in DNA repair, by complementation of an NER-defective *Mycobacterium smegmatis* Δ*uvrD1* strain with a series of biochemically-defined UvrD1 mutants. By assaying complemented strains for sensitivity to UVC, MMC, cisplatin, and psoralen–UVA, we conclude that monomeric UvrD1 ATPase activity suffices for the NER functions of UvrD1 *in vivo*. Decoupling ATP hydrolysis from duplex unwinding does not affect the repair activity of UvrD1, nor does interdiction of domain 2B cysteine disulfide-mediated dimerization or deletion of the Tudor domain. Our results militate against a proposed model in which UvrD1's repair function is governed by the redox state of the bacterium via its impact on UvrD1 dimerization and helicase activity.

Graphical abstract

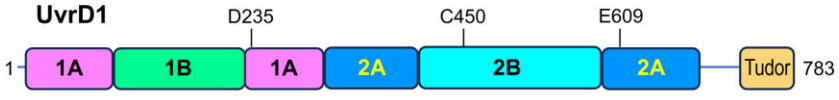

Complementation of *M. smegmatis* Δ*uvrD1* nucleotide excision repair

WT	monomeric ATPase / homodimeric helicase	YES
D235A	ATPase inactive / helicase inactive	NO
E609A	ATPase active / helicase inactive	YES
C450A	ATPase active / helicase inactive / obligate monomer	YES

Introduction

The nucleotide excision repair (NER) pathway driven by the UvrABC excinuclease complex has been extensively characterized in *Escherichia coli* and *Bacillus* [1] and is conserved in diverse bacterial taxa, including mycobacteria. The NER machinery locates and excises bulky DNA lesions such as short wave ultraviolet (UVC)-induced intra-strand cyclopyrimidine dimers (CPDs). The damage is recognized by a UvrA dimer, which recruits UvrB. After UvrA dissociates, UvrB sits on the lesion and recruits UvrC, a bifunctional endonuclease that incises the CPD-containing strand 7-nucleotides 5′ of the CPD (via UvrC's RNase-H like nuclease module) and 3–4 nucleotides 3′ of the CPD (via UvrC's GIY-YIG nuclease module) [2]. The UvrD ATPase (UvrD1 in mycobacteria) then displaces UvrC and the 12- to 13-mer CPD-containing oligonucleotide from the post-incision complex and the resulting gap is filled in by DNA polymerase and sealed by DNA ligase.

The NER system of mycobacteria has attracted attention in light of the findings that Δ*uvrB*, Δ*uvrD1*, and Δ*uvrA* Δ*uvrD1* mutants of *Mycobacterium tuberculosis* are attenuated with respect to virulence in mice [3, 4]. As expected, deletions of *uvrA*, *uvrB*, and *uvrD1* hypersensitize mycobacteria to killing by UVC [4–7, 8]. Early studies indicated that mycobacterial Δ*uvrA*, Δ*uvrB*, and Δ*uvrD1* strains were also sensitive to killing by mitomycin C (MMC) [4, 8]. MMC reacts with guanine bases at 5′-CpG sites to form inter-strand G-G crosslinks and G-monoadducts [9]. The connection between NER proteins and MMC damage was fortified by the findings that

Received: February 18, 2025. **Revised:** March 20, 2025. **Editorial Decision:** March 20, 2025. **Accepted:** March 24, 2025
© The Author(s) 2025. Published by Oxford University Press on behalf of Nucleic Acids Research.
This is an Open Access article distributed under the terms of the Creative Commons Attribution-NonCommercial License (https://creativecommons.org/licenses/by-nc/4.0/), which permits non-commercial re-use, distribution, and reproduction in any medium, provided the original work is properly cited. For commercial re-use, please contact reprints@oup.com for reprints and translation rights for reprints. All other permissions can be obtained through our RightsLink service via the Permissions link on the article page on our site—for further information please contact journals.permissions@oup.com.

MMC treatment of *Mycobacterium smegmatis* increased the expression of *uvrB* (by seven-fold), *uvrA* (three-fold), *uvrD1* (three-fold), and *uvrC* (two-fold) in a PafBC transcription factor-dependent fashion [10].

Our group has had a longstanding interest in *M. smegmatis* UvrD1 (a 783-aa polypeptide), having purified and characterized the enzyme biochemically and genetically in 2007 [5]. Mycobacterial UvrD1 has a C-terminal domain that mediates a physical interaction with the nonhomologous end joining (NHEJ) factor Ku, a double-strand break end-binding protein [5]. The monomeric form of UvrD1 protein is a vigorous DNA-dependent ATPase but a very weak 3′-to-5′ DNA helicase. Ku stimulates monomeric UvrD1 to catalyze ATP-dependent unwinding of 3′-tailed duplex DNA [5, 11]. According to AlphaFold 3 [12], a predicted C-terminal Tudor domain of UvrD1 is preceded by a disordered loop (aa 692–730) rich in serine, glycine, and proline that connects to the core ATPase motor, which consists of two RecA-like domains (1A and 2A) that bind ATP•Mg^{2+} and two accessory domains (1B and 2B) (Fig. 1A). The disordered loop has no apparent equivalent in *E. coli* UvrD or *Bacillus* PcrA [11]. Deleting the C-terminal 90-aa of *M. smegmatis* UvrD1 had no effect on UvrD1-(1–693)'s DNA-dependent ATPase activity or on UvrD1-(1–693) binding to a 3′-tailed duplex helicase substrate. Yet, the CΔ90 deletion diminished duplex unwinding in the presence of Ku and precluded formation of a stable DNA•UvrD1•Ku ternary complex [11].

The Lohman/Galburt group recently characterized a homodimeric version of UvrD1, formed via an inter-subunit cysteine disulfide linkage, that is a vigorous DNA helicase without Ku [13]. Their cryo-electron microscopy (cryo-EM) single-particle reconstruction models of dimeric and monomeric UvrD1 bound to 3′-tailed duplex DNAs (at 5–6 Å resolution) provide key evidence that the two UvrD1 protomers in the cysteine-linked dimer (formed by contacts between the 2B domains of the protomers) are arrayed in tandem on the 3′-tail with the lead protomer poised at the single-strand/duplex junction [14]. By contrast, the UvrD1 monomer engages the 3′-tail and junction in a different auto-inhibited conformation entailing DNA interactions of the 2B domain that are absent in the active homodimer•DNA structure. Chadda *et al.* [13] propose that UvrD1's repair function is tuned by the redox state of the cell, being triggered into action under oxidizing conditions. These new results and proposals make it acutely important to test genetically which physical and functional states of UvrD1 are relevant for its functions in DNA repair *in vivo*.

In light of previous findings that deletion of *M. smegmatis* Ku had no impact on sensitivity to killing by UVC [15], we envision that either: (i) the Ku-independent homodimeric UvrD1 helicase is the true agent of NER; or (ii) the monomeric UvrD1 ATPase suffices for NER and the homodimeric helicase activity is dispensable.

To distinguish between these scenarios, we conduct genetic complementation experiments whereby we express wild-type or mutant versions of UvrD1 in Δ*uvrD1* cells, achieved by inserting the *uvrD1* alleles at the chromosomal *attB* site under the control of the native *uvrD1* promoter [5]. We exploit UvrD1 mutants, including separation-of-function mutants, that were characterized biochemically with respect to DNA binding, ATP hydrolysis, and duplex unwinding [5, 11]. Domain 1A mutant D235A is ATPase-dead and helicase-dead, but fully competent for binding to the 3′-tailed duplex helicase substrate [5]. Domain 2A mutant E609A is fully active for DNA binding and ATP hydrolysis but is inactive in duplex unwinding on a 3′-tailed duplex substrate [11]. Mutants UvrD1-(1–729) and UvrD1-(1–693) retain ATPase and DNA binding functions but lack the predicted Tudor domain (the structure of which we solve here) and the Tudor plus linker domains, respectively. Most important, we test mutant C450A in which the domain 2B cysteine shown to mediate UvrD1 dimerization [13] (Fig. 1A) is replaced by alanine. This maneuver addresses the key question of whether cysteine disulfide-mediated dimerization is required for any or all of UvrD1's *in vivo* functions.

By assaying these complemented strains for sensitivity to multiple clastogens, we conclude that: (i) the monomeric UvrD1 ATPase activity suffices for all UvrD1 DNA repair functions *in vivo*; (ii) decoupling ATP hydrolysis from duplex unwinding by E609A does not affect UvrD1's DNA repair functions; (iii) cysteine disulfide-mediated dimerization plays no apparent DNA repair role *in vivo*; and (iv) the C-terminal Tudor domain and the linker segment are inessential for DNA repair *in vivo*. These results militate against a proposed model in which UvrD1 repair function is under redox control.

Materials and methods

Complementation of Δ*uvrD1* by expression of wild-type UvrD1 and UvrD1 mutants

DNA fragments encoding wild-type or mutated UvrD1 proteins under the control of the native *uvrD1* promoter (a 200-bp genomic DNA segment upstream of the translation start codon) were inserted between the NotI and HindIII sites of the integration-proficient plasmid pMV306-Kan that contains the bacteriophage L5 *attP–int* region and a kanamycin-resistance gene [16]. The pMV306-Kan-UvrD1 inserts were sequenced to verify that no unintended coding changes were acquired during amplification and cloning. The pMV306-Kan-UvrD1 plasmids were transformed into an *M. smegmatis* Δ*uvrD1* strain that has an in-frame deletion spanning amino acids 27–756 of the UvrD1 polypeptide [5]. Wild-type *uvrD1* and Δ*uvrD1* null cells were transformed in parallel with the empty pMV306-Kan vector. Integrants at the chromosomal *attB* site were selected on 7H10 agar plates containing 20 μg/ml kanamycin, 0.5% glycerol, 0.5% dextrose. The integrated *uvrD1* genes were polymerase chain reaction (PCR)-amplified using primers complementary to plasmid sequences flanking the open reading frame (ORF) and then sequenced to affirm the presence of the desired wild-type or mutated *uvrD1* alleles or, in the case of the vector control transformants, the integration of the vector.

Sensitivity to UVC irradiation

Mycobacterium smegmatis strains were grown to log phase (A_{600} 0.3–0.4) and serial 10-fold dilutions prepared in 7H9 media were spotted on 7H10 agar plates supplemented with 20 μg/ml kanamycin, 0.5% glycerol, 0.5% dextrose. UV irradiation at the doses specified in the figures was performed with a Spectrolinker XL-1500 UV crosslinker (Spectronic Corp.) fitted with 254 nm bulbs. Immediately after exposure, the plates were wrapped in foil (to prevent repair by photolyase) and incubated at 37°C for 3 days. UV sensitivity experiments were performed with three independent biological replicates; representative experiments are shown in Fig. 1B.

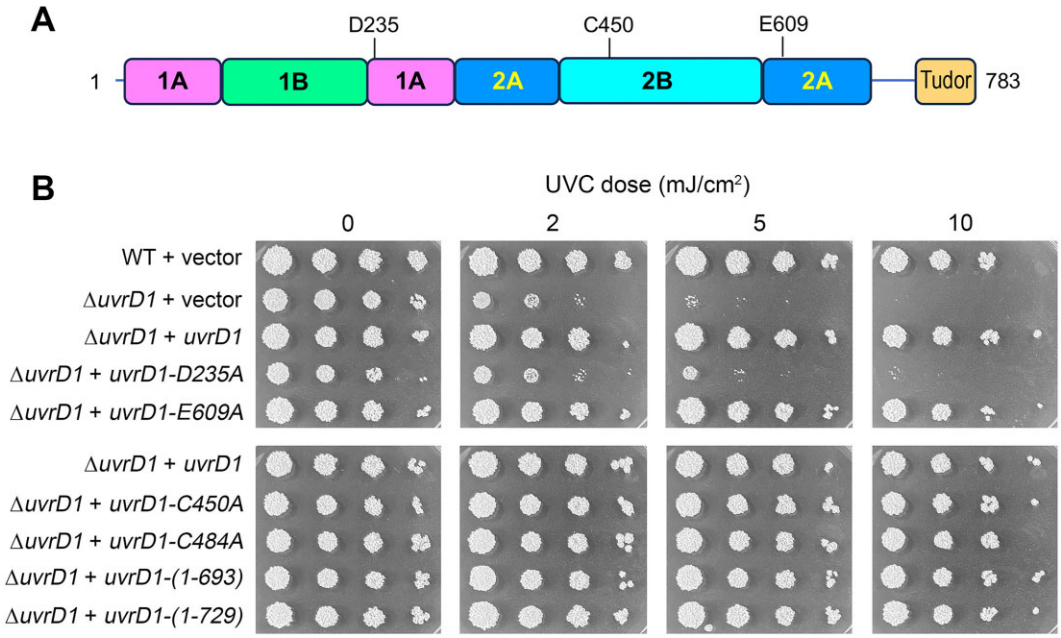

Figure 1. Complementation of Δ*uvrD1* UVC sensitivity by wild-type and mutant UvrD1s. (**A**) Schematic of the domain architecture of the *M. smegmatis* UvrD1 protein. RecA-like domains 1A and 2A form the ATP•Mg^{2+} binding site. Asp235 in domain 1A engages the divalent cation cofactor for ATP hydrolysis. Glu609 in domain 2A is essential for duplex unwinding albeit not for ATP hydrolysis [11]. A cysteine in domain 2B (Cys450 in *M. smegmatis* UvrD1) is responsible for cysteine disulfide-mediated dimerization of UvrD1 [13]. The C-terminal Tudor domain is implicated in UvrD1 interaction with Ku [5]. (**B**) Serial 10-fold dilutions of wild-type or Δ*uvrD1* cells with the indicated *uvrD1* alleles (or empty vector) inserted at the chromosomal *attB* locus were spotted on 7H10 agar plates, which were exposed to the UVC (254 nm) doses specified (0, 2, 5, or 10 mJ/cm^2). The plates were photographed after incubation in the dark for 3 days at 37°C.

Sensitivity to MMC

Log phase cultures (1.5 ml at A_{600} of 0.3–0.4) of *M. smegmatis* strains grown in 7H9 medium were supplemented with MMC (from Sigma; prepared as a 0.8 mg/ml stock solution in dimethylsulfoxide) at the concentrations specified in figure legends. After incubation for 2 h at 37°C with constant shaking (200 rpm), the control and MMC-treated cells were harvested by centrifugation, washed twice with drug-free 7H9 medium, and resuspended in 7H9 medium to attain equal optical density. Aliquots (2.5 µl) of serial 10-fold dilutions were spotted on 7H10 agar plates supplemented with 20 µg/ml kanamycin, 0.5% glycerol, 0.5% dextrose and incubated at 37°C for 3 days. MMC sensitivity experiments were performed with three independent biological replicates; representative experiments are shown in Figs 3 and 5.

Sensitivity to cisplatin

Log phase cultures (1.5 ml at A_{600} of 0.3–0.4) of *M. smegmatis* strains grown in 7H9 medium were supplemented with cisplatin (from US Pharmacopeia, prepared as a 2 mg/ml stock solution in 150 mM NaCl) at the concentrations specified in figure legends. After incubation for 1 h at 37°C with constant shaking (200 rpm), the control and cisplatin-treated cells were harvested by centrifugation, washed once with drug-free 7H9 medium, and resuspended in 7H9 medium to attain equal optical density. Aliquots (2.5 µl) of serial 10-fold dilutions were spotted on 7H10 agar plates supplemented with 20 µg/ml kanamycin, 0.5% glycerol, 0.5% dextrose, and incubated at 37°C for 3 days. Cisplatin sensitivity experiments were performed with three independent biological replicates; representative experiments are shown in Figs 3 and 5.

Sensitivity to trioxsalen–UVA

Log phase cultures (1.5 ml at A_{600} of 0.3–0.4) of *M. smegmatis* strains grown in 7H9 medium were diluted in 10-fold increments and aliquots (2.5 µl) were spotted on 7H10 agar plates supplemented with 0.1 µg/ml trioxsalen (from Thermo Scientific; prepared as a 1 mg/ml stock solution in dimethylsulfoxide), 20 µg/ml kanamycin, 0.5% glycerol, 0.5% dextrose. The agar plates were incubated at 37°C for 2 h to allow uptake of trioxsalen and then UVA-irradiated for the times specified with a 100W 365 nm LED lamp (Everbeam) placed 10 cm above the plate. Immediately after exposure, the plates were wrapped in foil and incubated at 37°C for 3 days. Trioxsalen sensitivity experiments were performed with three independent biological replicates; representative experiments are shown in Figs 3 and 4.

Sensitivity to angelicin–UVA

Log phase cultures (1.5 ml at A_{600} of 0.3–0.4) of *M. smegmatis* strains grown in 7H9 medium were supplemented with 20 µg/ml angelicin (from Sigma; prepared as a 1 mg/ml stock solution in ethanol). After incubation for 2 h at 37°C with constant shaking (200 rpm), the cells were serially 10-fold diluted in 7H9 medium containing 20 µg/ml angelicin. Aliquots (2.5 µl) of serial 10-fold dilutions were spotted on 7H10 agar plates supplemented with 0.5% glycerol, 0.5% dextrose. The agar plates were then UVA-irradiated for the times specified with a 100 W 365 nm LED lamp (Everbeam) placed 10 cm above the plate. Immediately after exposure, the plates were wrapped in foil and incubated at 37°C for 3 days. Angelicin sensitivity experiments were performed with three independent biological replicates; representative experiments are shown in Fig. 3.

Recombinant UvrD1 Tudor domain

The ORF encoding the C-terminal segment (aa 731–783) of *M. smegmatis* UvrD1 (Msmeg_5534) was PCR-amplified from genomic DNA with primers that introduced a BglII site upstream of aa 731 and a HindIII site downstream of the native stop codon. The PCR products were digested with BglII and HindIII and ligated into pET28b-His_{10}Smt3 that had been digested with BamHI and HindIII. The resulting pET28b-His_{10}Smt3-UvrD1-C plasmid encodes UvrD1-(731–783) fused to an N-terminal His_{10}Smt3 tag under the transcriptional control of a T7 RNA polymerase promoter. The pET28b-His_{10}Smt3-UvrD1-C plasmid was transformed into *E. coli* BL21(DE3) cells. Cultures (2-L) amplified from single kanamycin-resistant transformants were grown at 37°C in LB (Luria-Bertani) broth containing 60 μg/ml kanamycin until the A_{600} reached 0.7. The cultures were chilled on ice for 1 h, then adjusted to 2% (v/v) ethanol and 0.5 mM isopropyl-β-D-thiogalactopyranoside and incubated for 16 h at 18°C with constant shaking. All subsequent procedures were performed at 4°C. Cells were harvested by centrifugation and resuspended in 50 ml of buffer A (50 mM Tris–HCl, pH 8.0, 500 mM NaCl, 20 mM imidazole, 1 mM DTT (dithiothreitol), 20% glycerol) containing 1 protease inhibitor cocktail tablet (Roche). Lysozyme was added to a concentration of 1 mg/ml and the suspension was Dounce-homogenized prior to sonication to reduce viscosity. The insoluble material was pelleted by centrifugation at 38000g for 45 min. The supernatant was mixed for 1 h with 5 ml of Ni-NTA agarose resin (Qiagen) that had been equilibrated with buffer A. The resin was recovered by centrifugation and resuspended in 40 ml of buffer B (50 mM Tris–HCl, pH 8.0, 250 mM NaCl, 20 mM imidazole, 1 mM DTT, 10% glycerol). The resin was recovered by centrifugation and resuspended in 40 ml of buffer B. This wash step was repeated three times. The recovered resin was poured into a column. After washing the column with 30 ml of buffer B, the bound material was eluted with buffer C (50 mM Tris–HCl, pH 8.0, 250 mM NaCl, 500 mM imidazole, 1 mM DTT, 10% glycerol). The polypeptide compositions of the eluate fractions were monitored by sodium dodecyl sulfate–polyacrylamide gel electrophoresis. The eluate fractions containing His_{10}Smt3-UvrD1-(731–783) were pooled and supplemented with Smt3-specific protease Ulp1 [His_{10}Smt3-UvrD1-(731–783):Ulp1 ratio of 1000:1] and then dialyzed overnight in 1 l of buffer B. The tag-free UvrD1-(731–783) protein was then separated from His_{10}Smt3 by applying the dialysate to a 5-ml Ni-NTA agarose column that had been equilibrated with buffer B. The flow through fractions containing UvrD1-(731–783) were pooled, concentrated to 4 mg/ml by centrifugal ultrafiltration (Amicon filter, MWCO 3500 Da), and subjected to gel filtration through a 24-ml Superdex-200 column equilibrated in buffer D (25 mM Tris–HCl, pH 8.0, 150 mM NaCl, 1 mM DTT). Peak fractions were pooled, concentrated by centrifugal ultrafiltration, frozen, and stored at –80°C. Protein concentrations were determined with the BioRad dye reagent using bovine serum albumin as the standard. The yield was 1.5 mg of UvrD1-(731–783).

Structure of the UvrD1 Tudor domain

Crystals of UvrD1-(731–783) were grown by sitting drop vapor diffusion at 22°C. Aliquots (1 μl) of 430 μM UvrD1-(731–783) in buffer D were mixed with an equal volume of reservoir solution containing 0.2 M NaCl, 0.1 M Bis–Tris, pH 5.5, and 25% PEG-3350. Crystals were harvested and made into a seed stock using a seed bead kit (Hampton Research). Aliquots (1 μl) of 430 μM UvrD1-(731–783) were then mixed with 1 μl seed stock and 2 μl of reservoir solution containing 0.2 M NaCl, 0.1 M Bis–Tris, pH 5.5, and 25% PEG-3350. Crystals that grew after 2–4 days were cryoprotected in paraffin oil and then flash-frozen in liquid nitrogen. X-ray diffraction data from a single UvrD1-(731–783) crystal were collected at the Advanced Photon Source beamline 24-ID-C. The crystal diffracted to 2.59 Å resolution, belonged to space group $P22_12_1$, and contained five protomers in the asymmetric unit. Reduction of the crystallographic data were performed using XDS [17] and AIMLESS [18, 19]. The UvrD1-(731–783) structure was determined by molecular replacement, implemented in PHASER [20], using an AlphaFold predicted structure of UvrD1-(731–783) as the search model. The structure was iteratively improved in REFMAC [21] interspersed with manual adjustments of the model in COOT [22]. The refined model (R_{work}/R_{free} of 23.4/29.8) comprised continuous polypeptides from aa 731 to 781 for promoters B, C, D, and E. In protomer A, residues Gly766 and Ser767 at the tip of a β-hairpin loop were disordered. The crystallographic data collection information, refinement statistics, and model coordinates are available via the RCSB Protein Data Bank (PDB ID 9DQS; released 16 October 2024).

Results

UVC resistance requires UvrD1's ATPase but does not depend on chemomechanical coupling to DNA unwinding.

UVC exposure causes intra-strand DNA lesions—CPDs and 6–4 photoproducts—that are repaired in *M. smegmatis* via NER, as evinced by the exquisite sensitivity of Δ*uvrD1* cells *vis-à-vis* wild-type cells to killing by escalating doses (2, 5, or 10 mJ/cm^2) of 254 nm UV light. (Fig. 1B). UVC resistance was restored when the wild-type *uvrD1* gene, under the control of its native promoter, was inserted into the *attB* chromosomal locus of the Δ*uvrD1* strain (Fig. 1B). There was no rescue of UVC resistance by the *uvrD1-D235A* allele that encodes an ATPase-dead, helicase-dead version of UvrD1 that nonetheless retains activity in DNA binding [5] (Fig. 1B). Asp235, a constituent of superfamily 1 (SF1) helicase motif II (DExQ), coordinates the divalent cation cofactor for ATP hydrolysis [11]. By contrast, UVC resistance was fully complemented by the *uvrD1-E609A* allele that encodes an DNA binding-active, ATPase-active, helicase-dead version of UvrD1 [11] (Fig. 1B). Glu609, located in helicase motif V, is modeled to contact the ATP ribose 3′-OH and the motif IV Arg308 side chain that is essential for ATP hydrolysis; mutation of Glu609 to alanine uncouples ATP hydrolysis from duplex unwinding [11]. These results signify that ATP hydrolysis is essential for UvrD1 function in NER whereas duplex unwinding (as gauged by displacement of a 24-bp duplex with a 3′ single-strand tail) is not.

The UvrD1 C-terminal Tudor and linker modules are dispensable for UVC resistance

At the time of the initial characterization of UvrD1, the structure of the C-terminal domain of UvrD/PcrA-like helicases was not known. Here, we solved a 2.6 Å crystal structure of the 53-aa C-terminal segment of *M. smegmatis* UvrD1, from

aa 731–783, and found that it adopts a Tudor domain fold, comprising a 5-strand antiparallel β-barrel (PDB 9DQS; Fig. 2). This accords with structures determined for C-terminal Tudor domain folds in *Bacillus* PcrA, *E. coli* UvrD, and *Thermus* UvrD [23–25] (Fig. 2). The Tudor domain mediates interactions of UvrD/PcrA with RNA polymerase and UvrB [23–26]. It was suggested recently that the Tudor domain exerts an autoinhibitory effect on mycobacterial UvrD1's unwinding activity and that the interaction of Ku with the Tudor domain relieves this inhibition [27].

Here we tested complementation of the Δ*uvrD1* UVC sensitivity phenotype by introducing into *attB* the C-terminally truncated alleles *uvrD1-(1–729)*, which lacks the Tudor domain, and *uvrD1-(1–693)*, which lacks the disordered loop and the Tudor domain. Both truncated proteins restored UVC resistance to Δ*uvrD1* cells (Fig. 1B). Thus, any protein interactions imputed to the UvrD1 Tudor domain are deemed to be unnecessary for UvrD1's function in the repair of UVC damage.

Cysteine disulfide-mediated dimerization is dispensable for UVC resistance

Chadda *et al*. identified Cys451 in the 2B domain of *M. tuberculosis* UvrD1 as the residue responsible for cysteine disulfide-mediated dimerization of UvrD1 and the ensuing activation of the homodimeric UvrD1 helicase [13, 14]. The *M. tuberculosis* UvrD1-C451A mutant enzyme is exclusively monomeric, active as an ATP-dependent 3′-to-5′ translocase on single-strand DNA, but inactive as a helicase per se [13]. The equivalent cysteine residue in *M. smegmatis* UvrD1 is Cys450. We inserted into the *attB* chromosomal locus of the Δ*uvrD1* strain a *uvrD1-C450A* allele encoding a full-length UvrD1 protein that cannot form the cysteine disulfide linkage. Expression of UvrD1-C450A restored UVC resistance (Fig. 1B). We conclude that the cysteine disulfide-mediated UvrD1 homodimerization described by Chadda *et al*. [13, 14] is not pertinent to UvrD1's NER function *in vivo*. As a control we replaced Cys484 with alanine and found that the *uvrD1-C484A* allele also complemented the UVC sensitivity of the Δ*uvrD1* strain (Fig. 1B).

NER protects against DNA damage caused by MMC, cisplatin, and psoralen–UVA

Here we compared the effects of Δ*uvrD1* and Δ*uvrB* on sensitivity to three DNA-damaging agents that form a mixture of inter-strand crosslinks (ICLs) and base monoadducts. MMC reacts with guanine-N2 in the DNA minor groove at 5′-CpG sites to form inter-strand G-G crosslinks and G-monoadducts [9]. Cisplatin forms inter-strand G-G crosslinks, intra-strand G-G and G-A crosslinks, and G-monoadducts via reaction with purine-N7 in the major groove [28]. Trioxsalen is a bifunctional psoralen with two photoactive sites that intercalates into DNA and sequentially forms single-strand adducts and inter-strand crosslinks after photoactivation with 365 nm UV light (UVA), via cycloaddition to the 5,6 double bond of pyrimidines, preferentially at the thymine bases of 5′-TA dinucleotides [29]. We found that Δ*uvrD1* and Δ*uvrB* rendered *M. smegmatis* sensitive to killing by MMC, cisplatin, and trioxsalen–UVA (Fig. 3A). Δ*uvrB* cells were apparently more sensitive than Δ*uvrD1* cells to killing by MMC and cisplatin; this disparity was not evident with respect to killing by trioxsalen–UVA (Fig. 3A).

Angelicin is a monofunctional psoralen that, because of its angular structure, is unable to form ICLs and produces almost entirely monoadducts [30]. Studies in *E. coli* showed that Δ*uvrA*, Δ*uvrB*, and Δ*uvrC* mutants are hypersensitive to killing by angelicin [30], suggesting that angelicin-pyrimidine monoadducts are repaired via NER. To see if this is the case in mycobacteria, we tested *M. smegmatis* mutants lacking UvrB or UvrD1 for sensitivity to a 2-h exposure to 20 μg/ml angelicin in liquid medium, after which dilutions were spotted on agar medium and the plates were treated with UVA for 0, 1, 2, or 4 min. Survival was gauged after 3-day incubation at 37°C. In parallel, we tested the angelicin sensitivity of *M. smegmatis* mutants lacking Lhr and Nei2, which are encoded in a DNA damage-inducible *lhr–nei2* gene operon that protects *M. smegmatis* from killing by ICLs [31, 32]. Lhr is a 3′-to-5′ DNA helicase with a distinctive homotetrameric quaternary structure [33, 34]. Nei2 is a DNA glycosylase/lyase [31, 32]. Genetically interdicting the activity of the Lhr helicase sensitizes mycobacteria to killing by MMC, cisplatin, and trioxsalen–UVA. By contrast, the Nei2 glycosylase functions uniquely in evasion of damage caused by trioxsalen–UVA [31, 32]. Ablating Lhr and Nei2 does not sensitize *M. smegmatis* to UVC [31, 32].

We found that Δ*uvrD1* and Δ*uvrB* strains treated with angelicin were sensitive to killing by 2 and 4 min exposure to UVA, whereas the wild-type control and the Δ*lhr* and Δ*nei2* strains were virtually identical in their resistance to angelicin–UVA (Fig. 3B). Note that 4 min of UVA had no impact on any of the strains in the absence of prior treatment with angelicin. These results signify that Lhr and Nei2 are specifically dedicated to defense against psoralen ICLs and are not implicated in the repair of psoralen monoadducts, which are apparently substrates for NER via UvrD1 and UvrB. We infer that the sensitivity of Δ*uvrD1* and Δ*uvrB* cells to MMC and cisplatin arises because the NER machinery excises the purine base monoadducts generated by MMC and cisplatin.

UvrD1 repair of MMC, cisplatin, and psoralen–UVA damage depends on ATP hydrolysis but not on cysteine disulfide-mediated dimerization or duplex unwinding

The sensitivities of the Δ*uvrD1* strain to killing by trioxsalen–UVA (Fig. 4), and MMC and cisplatin (Fig. 5) were fully reversed by expression of either wild-type UvrD1, UvrD1-E609A, UvrD1-C450A, UvrD1-(1–729), or UvrD1-(1–693), all of which are ATPase-active, but not by the ATPase-dead UvrD1-D235A mutant.

Discussion

Simultaneous initial reports of the biochemical characterization of UvrD1 from *M. smegmatis* and *M. tuberculosis* [5, 35] described a vigorous monomeric single-stranded DNA (ssDNA)-dependent ATPase (K_m values of 110 μM and 63 μM ATP; k_{cat} values of 110 s^{-1} and 43 s^{-1}, respectively). The 3′-to-5′ helicase activity of *M. tuberculosis* UvrD1 on a variety of 3′-tailed duplex substrates was demonstrated under conditions of extreme enzyme excess (UvrD1:DNA molar ratio of 200:1 in most cases) [35]. Whereas *M. smegmatis* UvrD1 was unable to unwind a 3′-tailed duplex when present at two-fold excess over the helicase substrate, it quantitatively unwound the tailed duplex in the presence of a molar equivalent

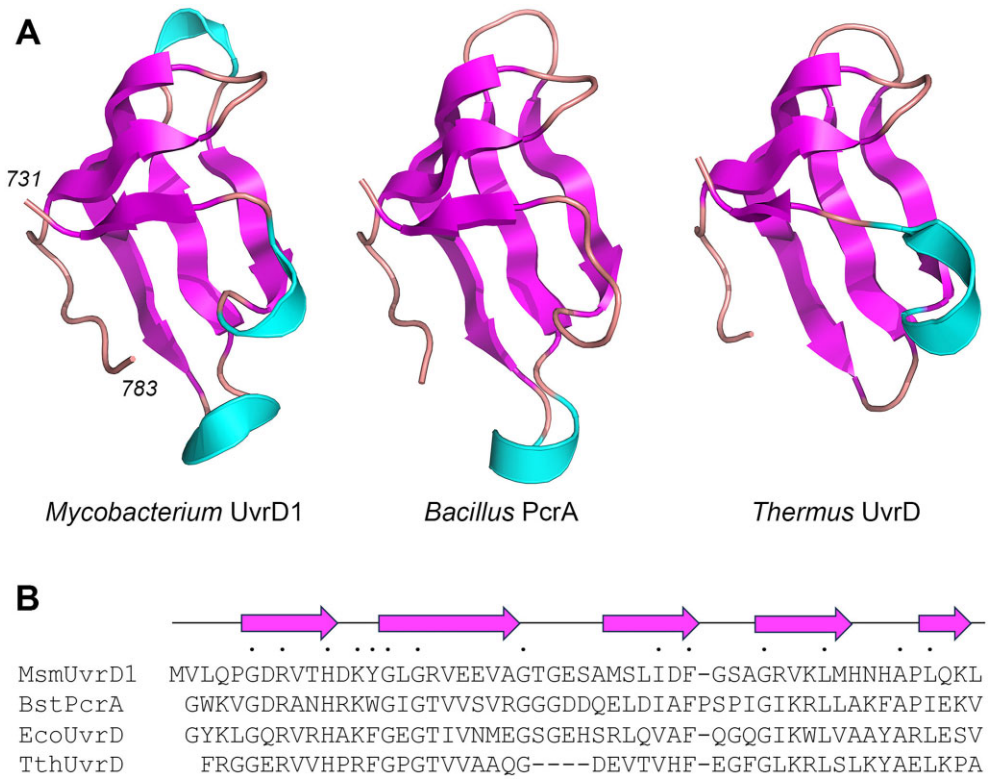

Figure 2. Structure of the C-terminal Tudor domain of UvrD1. (**A**) The tertiary structure of the *M. smegmatis* UvrD1 C-terminal Tudor domain (aa 731–783; PDB 9DQS) is depicted as a cartoon model with magenta β strands, flanked by the homologous Tudor domains of *Bacillus stearothermophilus* PcrA (PDB 5DMA) and *Thermus thermophilus* UvrD (PDB 7EGT). (**B**) Structure-based alignment of the primary structures of the Tudor domains of UvrD1, PcrA, and UvrDs from *T. thermophilus* and *E. coli*.

of Ku homodimer to UvrD1 [5]. EMSA assays established that monomeric UvrD1 per se binds the 3′-tailed duplex and recruits Ku to form a discrete higher order ternary complex [5, 11].

We now know via the work of Chadda *et al.* [13, 14, 27], that cysteine disulfide-mediated homodimerization of UvrD1 results in a highly active helicase per se, one that is much faster than the Ku-activated monomeric UvrD1 helicase. An obligate monomeric version of UvrD1 (by virtue of mutating the domain 2B cysteine to alanine) remains active as an ATP-dependent 3′-to-5′ translocase on single-strand DNA (at a rate of 130 nt•s^{-1}) but not as a DNA unwinding helicase [13]. These biochemical findings, along with recently reported cryo-EM structures of monomeric and homodimeric UvrD1 engaged on DNA [14], provide important new insights into helicase mechanism. Yet, the outstanding question is whether and how they bear on mycobacterial physiology and the role of UvrD1 in DNA repair.

The short answer is that they don't. To wit, by genetic complementation of the clastogen-sensitive *M. smegmatis* Δ*uvrD1* strain, we find that whereas the ATPase activity of UvrD1 is essential for UvrD1's NER function against base damage inflicted by UVC, MMC, cisplatin, and psoralen–UVA, UvrD1's repair activity is unaffected by mutations that uncouple ATP hydrolysis from duplex unwinding (E609A) or preclude disulfide-mediated homodimerization and hence helicase activity (C450A). Indeed, we show that the N-terminal ATPase domain per se (that lacks the C-terminal Tudor domain and the interdomain linker) suffices for UvrD1's NER function *in vivo*.

There is precedent for this scenario in the case of the essential mycobacterial DNA helicase UvrD2. UvrD2 is a monomeric protein with vigorous DNA-dependent ATPase and 3′-to-5′ DNA helicase activities in the absence of any accessory proteins [5]. The UvrD2 protein is essential for viability of *M. smegmatis* and *M. tuberculosis*, i.e. attempts to disrupt the *uvrD2* gene were unsuccessful unless a second copy of *uvrD2* was present elsewhere in the chromosome [36, 37]. UvrD2 has a distinctive architecture composed of an N-terminal SF1 ATPase/helicase domain and a C-terminal HRDC domain, connected by a CxxC-(14)-CxxC tetracysteine module. Whereas the UvrD2 HRDC domain is not required for ATPase or helicase activities *in vitro*, deletion of the tetracysteine module abolishes duplex unwinding while preserving ATP hydrolysis [36]. Single alanine mutations in the helicase domain of UvrD2 were identified that either: (i) abolished ATP hydrolysis and helicase activity; or (ii) abolished helicase activity without affecting DNA-dependent ATP hydrolysis or translocation on ssDNA (i.e. a motif V E508A mutation equivalent to E609A in UvrD1) [37]. When such biochemically defined UvrD2 mutants were deployed to test complementation of Δ*uvrD2* lethality in *M. tuberculosis*, it was discovered that neither the HRDC domain nor the tetracysteine module was needed, and that the ATPase activity of UvrD2 was essential for viability but the helicase activity was dispensable [37]. A potential role for the UvrD2 HRDC domain during mycobacteriophage infection of *M. abscessus* was suggested by the isolation of phage-resistant host mycobacteria bearing frame-shift or missense mutations in the *M. abscessus* UvrD2 HRDC domain [38].

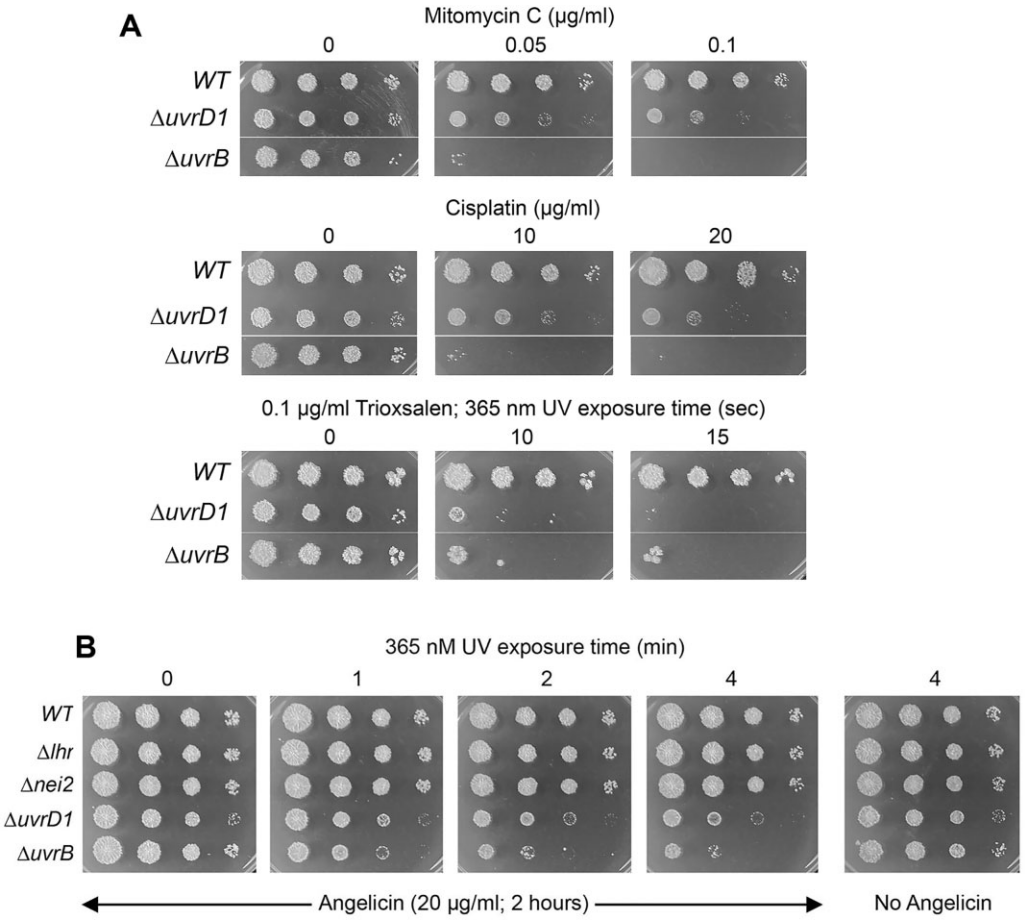

Figure 3. NER protects against DNA damage caused by MMC, cisplatin, and psoralen–UVA. (**A**) Sensitivity to MMC, cisplatin, and trioxsalen–UVA. Wild-type, Δ*uvrD1*, and Δ*uvrB* cells were treated with: (top panel) 0, 0.05, or 0.1 μg/ml MMC for 2 h at 37°C; or (middle panel) 0, 10, or 20 μg/ml cisplatin for 1 h at 37°C. After harvesting and washing to remove clastogen, serial 10-fold dilutions were spotted on 7H10 agar plates to gauge survival. (Bottom panel) Serial 10-fold dilutions of wild-type, Δ*uvrD1*, and Δ*uvrB* cells were spotted on 7H10 agar plates containing 0.1 μg/ml trioxsalen and then exposed to 365 nm light for 0, 10, or 15 s. The plates were photographed after incubation for 3 days at 37°C. (**B**) Sensitivity to angelicin–UVA. Wild-type, Δ*lhr*, Δ*nei2*, Δ*uvrD1*, and Δ*uvrB* cells were treated with 20 μg/ml angelicin for 2 h at 37°C, after which serial 10-fold dilutions were spotted on 7H10 agar plates and exposed to 365 nm light for 0, 1, 2, or 4 min. Control cells that had not been treated with angelicin were spotted in parallel and exposed to 365 nm light for 4 min. The plates were photographed after incubation for 3 days at 37°C.

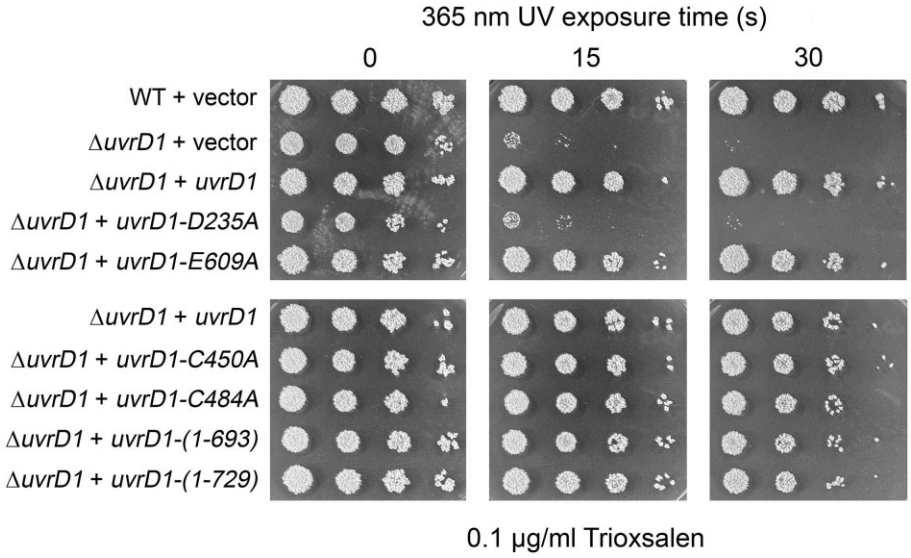

Figure 4. Complementation of Δ*uvrD1* trioxsalen–UVA sensitivity by wild-type and mutant UvrD1s. Serial 10-fold dilutions of wild-type or Δ*uvrD1* cells with the indicated *uvrD1* alleles (or empty vector) inserted at the chromosomal *attB* locus were spotted on 7H10 agar plates containing 0.1 μg/ml trioxsalen and then exposed to 365 nm light for 0, 15, or 30 s. The plates were photographed after incubation for 3 days at 37°C.

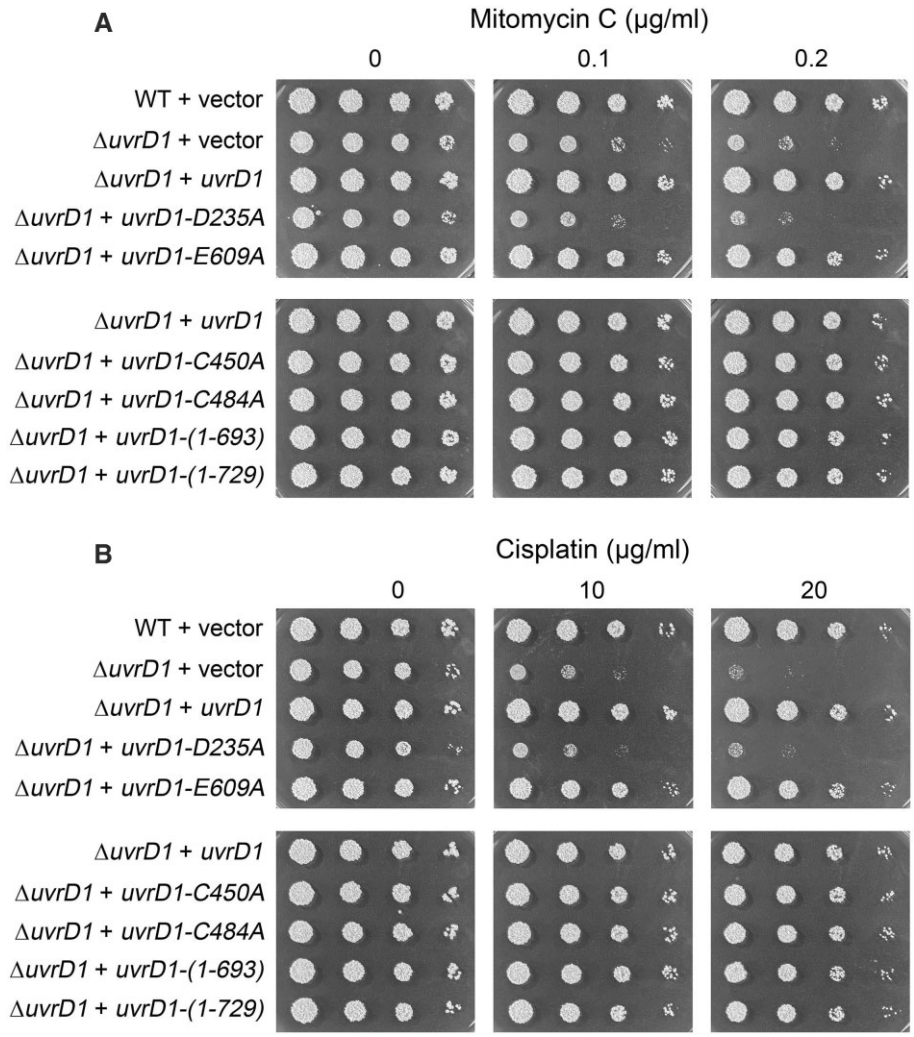

Figure 5. Complementation of Δ*uvrD1* MMC and cisplatin sensitivity by wild-type and mutant UvrD1s. Serial 10-fold dilutions of wild-type or Δ*uvrD1* cells with the indicated *uvrD1* alleles (or empty vector) inserted at the chromosomal *attB* locus were treated with: (**A**) 0, 0.1, or 0.2 μg/ml MMC for 2 h at 37°C; or (**B**) 0, 10, or 20 μg/ml cisplatin for 1 h at 37°C. After harvesting and washing to remove clastogen, serial 10-fold dilutions were spotted on 7H10 agar plates to gauge survival.

Our findings here that the UvrD1 C-terminal Tudor domain is inessential for mycobacterial NER resonate with studies of *E. coli* UvrD which showed that: (i) a truncated UvrD-(1–647) protein lacking the Tudor domain was active in displacing UvrC and a 12-mer lesion-containing oligonucleotide from the post-incision complex during NER *in vitro*; and (ii) expression of UvrD-(1–647) in *E. coli* Δ*uvrD1* cells restored resistance to killing by UVC up to 15 J/m^2 [39].

In conclusion, it is now evident that UvrD1 does not have to be either a cysteine-linked dimer or a helicase (as defined by standard helicase assays) to fulfill its NER functions *in vivo*. We feel that our genetic results weigh against a model [13] whereby UvrD1 activity in DNA repair is governed by the redox state of the cell via its impact on UvrD1 dimerization.

Of course, we cannot exclude the prospect that cysteine disulfide-mediated homodimerization and duplex unwinding are relevant to some hypothetical *in vivo* function of UvrD1 other than NER. In *E. coli*, UvrD plays a key role in the methyl-directed mismatch repair pathway spearheaded by MutL, MutS, and MutH, whereby interaction with MutL stimulates UvrD helicase activity and its displacement of the nicked mismatched strand [40, 41]. Yet, this scenario does not apply in mycobacteria, which lack the MutL/MutS system and instead rely on a distinct mechanism of mismatch repair catalyzed by the endonuclease NucS [42].

Acknowledgements

Author contributions: Garrett M. Warren (Conceptualization, Investigation, Writing—review & editing), Stewart Shuman (Conceptualization, Funding acquisition, Writing—original draft)

Conflict of interest

None declared.

Funding

U.S. National Institutes of Health Grant AI64693 (S.S.). The MSKCC structural biology core is supported by NCI Grant P30CA008748.

Data availability

The model coordinates of the UvrD1 Tudor domain are available via the RCSB Protein Data Bank (PDB ID 9DQS; released 16 October 2024).

References

1. Kisker C, Kuper J, Van Houten B. Prokaryotic nucleotide excision repair. *Cold Spring Harb Perspect Biol* 2013;**5**:a012591. https://doi.org/10.1101/cshperspect.a012591
2. Selby CP, Lindsey-Boltz LA, Yang Y *et al.* Mycobacteria excise DNA damage in 12- or 13-nucleotide-long oligomers by prokaryotic-type dual incisions and performs transcription-coupled repair. *J Biol Chem* 2020;**295**:17374–80. https://doi.org/10.1074/jbc.AC120.016325
3. Darwin KH, Nathan CF. Role for nucleotide excision repair in virulence of *Mycobacterium tuberculosis*. *Infect Immun* 2005;**73**:4581–7. https://doi.org/10.1128/IAI.73.8.4581-4587.2005
4. Houghton J, Townsend C, Williams AR *et al.* Important role for *Mycobacterium tuberculosis* UvrD1 in pathogenesis and persistence apart from its function in nucleotide excision repair. *J Bacteriol* 2012;**194**:2916–23. https://doi.org/10.1128/JB.06654-11
5. Sinha KM, Stephanou NC, Gao F *et al.* Mycobacterial UvrD1 is a Ku-dependent DNA helicase that plays a role in multiple DNA repair events, including double-strand break repair. *J Biol Chem* 2007;**282**:15114–25. https://doi.org/10.1074/jbc.M701167200
6. Kurthkoti K, Kumar P, Jain R *et al.* Important role of the nucleotide excision repair pathway in *Mycobacterium smegmatis* in conferring protection against commonly encountered DNA-damaging agents. *Microbiology* 2008;**154**:2776–85. https://doi.org/10.1099/mic.0.2008/019638-0
7. Rossi F, Khanduja JS, Bortoluzzi A *et al.* The biological and structural characterization of *Mycobacterium tuberculosis* UvrA provides novel insights into its mechanism of action. *Nucleic Acids Res* 2011;**39**:7316–28. https://doi.org/10.1093/nar/gkr271
8. Guthlein C, Wanner RM, Sander P *et al.* Characterization of the mycobacterial NER system reveals novel functions of the *uvrD1* helicase. *J Bacteriol* 2009;**191**:555–62. https://doi.org/10.1128/JB.00216-08
9. Paz MM, Ladwa S, Champeil E *et al.* Mapping DNA adducts of mitomycin C and decarbamoyl mitomycin C in cell lines using liquid chromatography/electrospray tandem mass spectrometry. *Chem Res Toxicol* 2008;**21**:2370–8. https://doi.org/10.1021/tx8002615
10. Muller AU, Imkamp F, Weber-Ban E. The mycobacterial LexA/RecA-independent DNA damage response is controlled by PafBC and the pup-proteasome system. *Cell Rep* 2018;**23**:3551–64. https://doi.org/10.1016/j.celrep.2018.05.073
11. Sinha KM, Glickman MS, Shuman S. Mutational analysis of *Mycobacterium* UvrD1 identifies functional groups required for ATP hydrolysis, DNA unwinding, and chemomechanical coupling. *Biochemistry* 2009;**48**:4019–30. https://doi.org/10.1021/bi900103d
12. Abramson J, Adler J, Dunger J *et al.* Accurate structure prediction of biomolecular interactions with AlphaFold 3. *Nature* 2024;**630**:493–500.
13. Chadda A, Jensen D, Tomko EJ *et al. Mycobacterium tuberculosis* DNA repair helicase UvrD1 is activated by redox-dependent dimerization via a 2B domain cysteine. *Proc Natl Acad Sci USA* 2022;**119**:e2114501119.
14. Chadda A, Nguyen B, Lohman TM *et al.* Structural basis for dimerization and activation of UvrD-family helicases. *Proc Natl Acad Sci USA* 2025;**122**:e2422330122. https://doi.org/10.1073/pnas.2422330122
15. Stephanou NC, Gao F, Bongiorno P *et al.* Mycobacterial nonhomologous end joining mediates mutagenic repair of chromosomal double-strand DNA breaks. *J Bacteriol* 2007;**189**:5237–46. https://doi.org/10.1128/JB.00332-07
16. Lee MH, Pascopella L, Jacobs WR *et al.* Site-specific integration of mycobacteriophage L5: integration-proficient vectors for *Mycobacterium smegmatis*, *Mycobacterium tuberculosis*, and bacille Calmette-Guérin. *Proc Natl Acad Sci USA* 1991;**88**:3111–5. https://doi.org/10.1073/pnas.88.8.3111
17. Kabsch W. XDS. *Acta Crystallogr D Biol Crystallogr* 2010;**66**:125–32. https://doi.org/10.1107/S0907444909047337
18. Collaborative Computational Project, Number 4. The CCP4 suite: programs for protein crystallography. *Acta Crystallogr D Biol Crystallogr* 1994;**50**:760–3. https://doi.org/10.1107/S0907444994003112
19. Evans PR, Murshudov GN. How good are my data and what is the resolution? *Acta Crystallogr D Biol Crystallogr* 2013;**69**:1204–14. https://doi.org/10.1107/S0907444913000061
20. McCoy AJ, Grosse-Kunstleve RW, Adams PD *et al.* Phaser crystallographic software. *J Appl Crystallogr* 2007;**40**:658–74. https://doi.org/10.1107/S0021889807021206
21. Murshudov GN, SkubaÃÅk P, Lebedev AA *et al.* REFMAC5 for the refinement of macromolecular crystal structures. *Acta Crystallogr D Biol Crystallogr* 2011;**67**:355–67. https://doi.org/10.1107/S0907444911001314
22. Emsley P, Cowtan K. Coot: model-building tools for molecular graphics. *Acta Crystallogr D* 2004;**60**:2126–32. https://doi.org/10.1107/S0907444904019158
23. Sanders K, Lin CL, Smith AJ *et al.* The structure and function of an RNA polymerase interaction domain in the PcrA/UvrD helicase. *Nucleic Acids Res* 2017;**45**:3875–87. https://doi.org/10.1093/nar/gkx074
24. Kawale AA, Burmann BM. UvrD helicase-RNA polymerase interactions are governed by UvrD's carboxy-terminal Tudor domain. *Commun Biol* 2020;**3**:607.
25. Bharati BK, Gowder M, Zheng F *et al.* Crucial role and mechanism of transcription-coupled DNA repair in bacteria. *Nature* 2022;**604**:152–9.
26. Urrutia-Irazabal I, Ault JR, Sobott F *et al.* Analysis of the PcrA-RNA polymerase complex reveals a helicase interaction motif and a role for PcrA/UvrD helicase in the suppression of R-loops. *eLife* 2021;**10**:e68829.
27. Chadda A, Kozlov AG, Nguyen B *et al. Mycobacterium tuberculosis* ku stimulates multi-round DNA unwinding by UvrD1 monomers. *J Mol Biol* 2024;**436**:168367. https://doi.org/10.1016/j.jmb.2023.168367
28. Ghosh S. Cisplatin: the first metal based anticancer drug. *Bioorg Chem* 2019;**88**:102925. https://doi.org/10.1016/j.bioorg.2019.102925
29. Zhen WP, Buchardt O, Nielsen H *et al.* Site specificity of psoralen-DNA interstrand cross-linking determined by nuclease Bal31 digestion. *Biochemistry* 1986;**25**:6598–603. https://doi.org/10.1021/bi00369a039
30. Perera AV, Mendenhall JB, Courcelle CT *et al.* Cho endonuclease functions during DNA interstrand cross-link repair in *Escherichia coli*. *J Bacteriol* 2016;**198**:3099–108. https://doi.org/10.1128/JB.00509-16
31. Warren GM, Ejaz A, Fay A *et al.* Mycobacterial helicase lhr abets resistance to DNA crosslinking agents mitomycin C and cisplatin. *Nucleic Acids Res* 2023;**51**:218–35. https://doi.org/10.1093/nar/gkac1222
32. Warren GM, Shuman S. Structure and *in vivo* psoralen DNA crosslink repair activity of mycobacterial Nei2. *mBio* 2024;**15**:e0124824. https://doi.org/10.1128/mbio.01248-24
33. Ejaz A, Ordonez H, Jacewicz A *et al.* Structure of mycobacterial 3′-to-5′ RNA:DNA helicase lhr bound to a ssDNA tracking strand highlights distinctive features of a novel family of bacterial helicases. *Nucleic Acids Res* 2018;**46**:442–55. https://doi.org/10.1093/nar/gkx1163

34. Warren GM, Wang J, Patel DJ *et al.* Oligomeric quaternary structure of *Escherichia coli* and *Mycobacterium smegmatis* lhr helicases is nucleated by a novel C-terminal domain composed of five winged-helix modules. *Nucleic Acids Res* 2021;**49**:3876–87. https://doi.org/10.1093/nar/gkab145
35. Curti E, Smerdon SJ, Davis EO. Characterization of the helicase activity and substrate specificity of *Mycobacterium tuberculosis* UvrD. *J Bacteriol* 2007;**189**:1542–55. https://doi.org/10.1128/JB.01421-06
36. Sinha KM, Stephanou NC, Unciuleac MC *et al.* Domain requirements for DNA unwinding by mycobacterial UvrD2, an essential DNA helicase. *Biochemistry* 2008;**47**:9355–64. https://doi.org/10.1021/bi800725q
37. Williams A, Güthlein C, Beresford N *et al.* UvrD2 is essential in *Mycobacterium tuberculosis*, but its helicase activity is not required. *J Bacteriol* 2011;**193**:4487–94. https://doi.org/10.1128/JB.00302-11
38. Dedrick RM, Smith BE, Garlena RA *et al. Mycobacterium abscessus* strain morphotype determines phage susceptibility, the repertoire of therapeutically useful phages, and phage resistance. *mBio* 2021;**12**:e03431–20. https://doi.org/10.1128/mBio.03431-20
39. Manelyte L, Guy CP, Smith RM *et al.* The unstructured C-terminal extension of UvrD interacts with UvrB, but is dispensable for nucleotide excision repair. *DNA Repair (Amst)* 2009;**8**:1300–10. https://doi.org/10.1016/j.dnarep.2009.08.005
40. Matson SW, Robertson AB. The UvrD helicase and its modulation by the mismatch repair protein MutL. *Nucleic Acids Res* 2006;**34**:4089–97. https://doi.org/10.1093/nar/gkl450
41. Liu J, Lee R, Britton BM *et al.* MutL sliding clamps coordinate exonuclease-independent *Escherichia coli* mismatch repair. *Nat Commun* 2019;**10**:5294. https://doi.org/10.1038/s41467-019-13191-5
42. Castañeda-Garcia A, Prieto AI, Rodríguez-Beltrán J *et al.* A non-canonical mismatch repair pathway in prokaryotes. *Nat Commun* 2017;**8**:14246. https://doi.org/10.1038/ncomms14246

Received: February 18, 2025. **Revised:** March 20, 2025. **Editorial Decision:** March 20, 2025. **Accepted:** March 24, 2025
© The Author(s) 2025. Published by Oxford University Press on behalf of Nucleic Acids Research.
This is an Open Access article distributed under the terms of the Creative Commons Attribution-NonCommercial License (https://creativecommons.org/licenses/by-nc/4.0/), which permits non-commercial re-use, distribution, and reproduction in any medium, provided the original work is properly cited. For commercial re-use, please contact reprints@oup.com for reprints and translation rights for reprints. All other permissions can be obtained through our RightsLink service via the Permissions link on the article page on our site—for further information please contact journals.permissions@oup.com.